Observation of vortex lattice melting in twinned $YBa_2Cu_3O_{7-x}$ using neutron small-angle scattering

C. M. Aegerter
Physik-Institut, Universität Zürich, CH-8057 Zürich, Switzerland

S. T. Johnson,* W. J. Nuttall,† S. H. Lloyd, M. T. Wylie, M. P. Nutley, and E. M. Forgan
School of Physics and Space Research, University of Birmingham, Birmingham B15 2TT, United Kingdom

R. Cubitt
Institut Laue Langevin, Grenoble, France

S. L. Lee
School of Physics and Astronomy, University of St. Andrews, St. Andrews, Fife KY169SS, United Kingdom

D. McK. Paul
Department of Physics, University of Warwick, Coventry CV4 7AL, United Kingdom

M. Yethiraj and H. A. Mook
Solid State Division, Oak Ridge National Laboratory, Oak Ridge, Tennessee 37831-6033

(Received 24 October 1997)

A neutron small-angle scattering study of the flux-line lattice in heavily twinned $YBa_2Cu_3O_{7-x}$ is presented. It is found that the diffraction signal disappears at temperatures well below T_c, associated with a melting of the flux lattice. The shape of the melting line is consistent with both a Lindemann criterion and the scaling expected for a vortex-glass transition with the superconducting parameters from the three-dimensional *XY* model. The influence of twin planes on the structure of the vortex lattice and its melting is studied by applying the field at different angles to the *c* axis. The results are compared with recent specific heat measurements on similar crystals. [S0163-1829(98)03022-7]

I. INTRODUCTION

High-temperature superconductors (HTS's) are, in many respects, different from classic type-II superconductors. This is due to several factors, including the layered structure resulting in highly anisotropic superconducting behavior. Moreover, HTS's have very short coherence lengths leading to extreme type-II behavior. The combination of these factors together with the high operating temperatures can produce exotic vortex phases such as the vortex-glass and the vortex-liquid phases.[1] Over the past few years, these vortex phases have been intensively studied in various compounds, particularly in the model low- and high-anisotropy systems $YBa_2Cu_3O_{7-x}$ (YBCO) and $Bi_2Sr_2CaCu_2O_{8+\delta}$ (BSCCO). Until recently, the phenomenon of flux-line lattice (FLL) or vortex-glass melting in YBCO has only been observed by magnetization and transport measurements.[2,3] This is because the vortex behavior is strongly influenced by the presence of twin-plane boundaries acting as strong, extended pinning sites and untwinned single crystals of sufficient size and quality have only recently become available. This is in contrast to BSCCO, in which there are no twin planes and where small-angle neutron scattering[4] (SANS) and muon spin rotation[5,6] (μSR) have both demonstrated the existence of a melting transition some years ago. Recently, a first-order melting transition has been observed using differential thermal analysis[7] (DTA) on an untwinned crystal also used in magnetization and transport measurements.[3] There have also been highly sensitive specific heat measurements on heavily twinned crystals of different purity.[8,9] In the samples of a purity similar to those used in the present work, a jump in specific heat, consistent with a second-order phase transition, was found over a certain range of fields. For the very-high-purity crystals studied, a similar jump was found; however, on increasing the field a peak in specific heat, consistent with a first-order transition, could be observed.[9] In this paper we present small-angle neutron scattering measurements on a heavily twinned YBCO crystal of a purity similar to those studied in Ref. 10, containing about 10% of nonsuperconducting inclusions (green phase).

In addition to the usual orientation of the field parallel to the *c* direction, we applied the field at an angle of 51° to the *c* axis and at 45° to the twin planes running along both a $\langle 110\rangle$ and a $\langle 1\bar{1}0\rangle$ direction (see Fig. 1). This is done in order to minimize the influence of the pinning to the twin planes on the vortex behavior. Such an arrangement has previously been shown to markedly influence the structure of the FLL. With the field parallel to the twin planes (and hence the *c* direction) a fourfold symmetry has been observed previously, which has been attributed to the strong pinning effects of the twin planes combined with that of *ab* anisotropy.[11,12] Alternatively, such a morphology has been claimed to arise from *d*-wave effects.[13] By applying the field

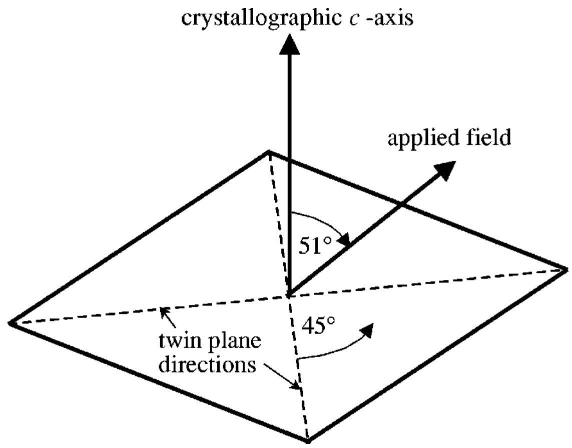

FIG. 1. Schematic representation of the alignment of the field with respect to the crystallographic axes. The twin boundaries run at 45° to the *a* and *b* axes. To minimize the effect of pinning by twin planes, the field is applied at 51° to the *c* axis, while at 45° to the twin boundaries.

at angles to the twin planes greater than the depinning angle (~25°), a morphology with two triangular lattices, distorted by the superconducting *ac* anisotropy was found.[13,14] This change in the FLL structure can be clearly seen by comparing Figs. 2 and 3, which show typical neutron diffraction pictures for the two cases. For both orientations, we observe the disappearance of the diffraction signal at temperatures well below T_c. In this way we map the melting line over the field range 0.5–4.5 T. These results agree well with the irreversibility temperatures measured using a vibrating sample magnetometer on a small piece of the same crystal. Further discussion in Sec. III compares these results to those obtained in the recent specific heat measurements by Roulin *et al.*[10]

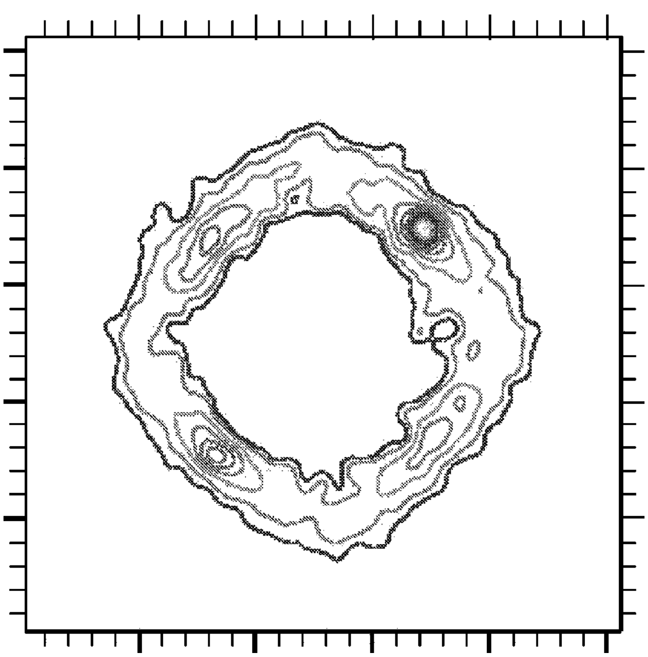

FIG. 2. Typical diffraction pattern with the field parallel to the *c* direction. The temperature was ~5 K, while the field was at 2 T. The diffraction pattern shows a fourfold symmetry, arising from the strong pinning to the twin planes (see the text) (Ref. 11).

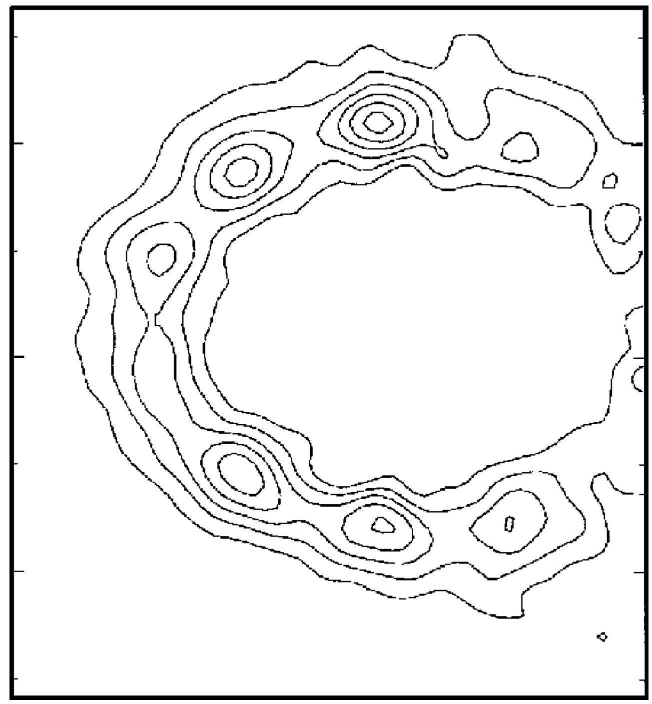

FIG. 3. Typical diffraction pattern with the field away from the twin planes (at 51° to the *c* axis). The temperature was 5 K and the field was 1.5 T. Only the left-hand side of the diffraction pattern fulfills the Bragg condition and can be seen. The picture clearly shows two hexagonal FLL's distorted by the anisotropy. The effect of the twin planes is thus much reduced, although the orientation of two spots from each FLL is still aligned with the twin boundaries (see the text).

II. EXPERIMENTAL DETAILS

The experiments were carried out using the instrument D17 at the ILL, Grenoble, France. The neutron beam, collimated over a distance of 2.75 m with a wavelength λ_n of typically 1.2 nm, was incident on the sample mounted in a horizontal-field cryomagnet capable of sample temperatures down to 1.5 K and a maximum field of 5 T. The scattered neutrons were detected by a position sensitive detector (approximately 0.8×0.8 m^2 total area with a pixel size of ~10 mm) and located at a distance from the sample that was varied between 2.88 and 3.43 m, depending on the applied field. The field was initially aligned with the neutron beam, to an accuracy of 0.1° both vertically and horizontally, by observing the diffraction pattern from the FLL in Nb. The sample was then aligned with the field either parallel or at 51° to the crystallographic *c* axis (see Fig. 1), by rotating the sample about the vertical axis.

The sample consisted of a large YBCO single crystal, of mass 7.8 g, grown using a melt processing technique. Measurements from an inductance coil mounted near the sample during the neutron experiments gave a value for T_c of $\simeq$92 K. The small-angle neutron scattering data reported in this paper were obtained during three experimental periods at the D17 diffractometer. Data from the first experiment have been published separately[15] and were obtained with the cryostat heater mounted on the sample stick. In the subsequent experiments the heating and thermometry were improved by placing the cryostat heater on the heat exchanger itself.

These changes of sample environment give rise to a small (approximately 1 K) discrepancy between the Pt resistance thermometer readings in the first experiment and those from later measurements. The critical temperature determined *in situ* in all cases, however, gives an independent calibration for the thermometry in the different setups. For this reason, the results presented below will always be given in terms of the reduced temperature $t = T/T_c$, with T_c determined in each case by measuring the inductance at 1 kHz of a coil placed near the sample.

A brief consideration of small-angle scattering from a FLL is now given. Typical FLL plane spacings are $\sim$50 nm (corresponding to a field of $\sim$1 T). Thus the FLL can only be observed by using small angles and long wavelengths. In our experiments we used wavelengths between 1.2 and 1.5 nm, depending on the applied field. Using these typical values, we obtain scattering angles $2\theta \simeq 2°$ from the Bragg condition

$$\lambda_n = 2 d_{hk} \sin(\theta), \tag{1}$$

where d_{hk} is the layer spacing. Due to its magnetic moment ($\mu_n = -1.913\mu_N$) a neutron may interact not only with the nuclei in a sample, but also with magnetic inhomogeneities. This allows the observation of FLL's in superconductors with small-angle neutron scattering.[16,17] The intensity of scattered neutrons in a Bragg reflection, integrated over angle as the sample is rocked through the Bragg condition (rocking curve) may then be calculated from the magnetic cross section to be[4]

$$I_{hk} = \frac{\pi \mu_n^2 \phi \lambda_n^2 V}{8 \Phi_0^2 \tau_{hk}} |F(\tau_{hk})|^2, \tag{2}$$

where ϕ is the flux of incoming neutrons, V is the sample volume, and $\Phi_0 = h/2e$ is the magnetic flux quantum. The magnetic form factor $F(\tau_{hk})$ is a measure of the τ_{hk} Fourier component of the spatial variation of the magnetic field in the sample and can be easily calculated for an extreme type-II superconductor in the London approximation. Due to their long penetration depths and short coherence lengths, HTS's are extremely type II and one obtains

$$F(\tau_{hk}) = \frac{B}{1 + \lambda^2 \tau_{hk}^2}. \tag{3}$$

Here λ is the (temperature-dependent) magnetic penetration depth and B is the average induction. Thus, for fields greater than B_{c_1}, corresponding to $\lambda \tau_{hk} > 1$, the scattered intensity depends on the penetration depth of the sample as $I \propto \lambda^{-4}$. Since the HTS's have very long penetration depths ($\lambda_{ab} \sim 150$–200 nm at low temperature and even longer close to T_c) the scattered intensities are very weak compared to conventional type-II superconductors.

Due to these difficulties, intrinsic in neutron scattering studies of HTS's, long counting times were required. Furthermore, there is very strong background scattering from extended defects in the sample. To obtain clear scattering images from the FLL in the sample, we subtracted a background measurement taken above the transition temperature T_c. Due to thermal contractions of the cryostat and sample stick, this background was numerically shifted by a fraction of a detector pixel in order to obtain good subtractions near the beam stop. Typical counting times were 1 h each for a foreground and a background.

III. RESULTS AND DISCUSSION

A typical diffraction pattern for the field parallel to the c axis is shown in Fig. 2, at low temperatures and a field of 2 T. There is a distinct fourfold symmetry visible in the scattering. This should not, however, be interpreted as the observation of a square lattice. As pointed out earlier,[13,14] measurements performed on similar crystals using higher resolution were able to distinguish 24 diffraction peaks corresponding to four different orientations of a *hexagonal* lattice. All of these orientations, corresponding to different domains in the sample, have strong diffraction peaks at 45° to the horizontal, consistent with strong pinning of FLL planes to twin boundaries. The different FLL orientations with the same strong 45° spots correspond to different orientations of the crystallographic a and b axes due to twinning.[11,12] The slight distortion from an ideal hexagonal lattice for the different orientations can then be understood as due to the small ab anisotropy present in YBCO. It can thus be seen that the main features of the FLL in the case where the field is parallel to the c axis is determined by the twin boundaries.

In the case of an inclined field (at 51° to the c axis), the situation is drastically changed. This is shown in Fig. 3, where a typical diffraction pattern at low temperatures and a field of 1.5 T is shown. The figure does not show a full diffraction pattern, as the scattering angles of the farthest spots differ by more than the width of the rocking curve. Therefore, the left-hand side of the pattern was deliberately illuminated by rocking close to the Bragg condition for spots on that side. One can clearly see six Bragg peaks on the left half, showing a distorted hexagonal symmetry. Taking the right-hand side of the pattern into account, this results in 12 spots corresponding to two orientations of a hexagonal lattice distorted by ac anisotropy. Assuming that the heavy twinning in our sample results in an effectively isotropic ab plane, this distortion can be parametrized by the ratio of the minor (α) and major (β) axes of the ellipse on which Bragg spots are situated. This should scale with angle as

$$(\alpha/\beta)^2 = \cos(\vartheta)^2 + 1/\gamma^2 \sin(\vartheta)^2, \tag{4}$$

where ϑ is the angle between the field and the c axis and $\gamma = \lambda_c/\lambda_{ab}$ parametrizes the anisotropy. For an angle of 51°, this scaling function is still determined almost entirely by the cosine term. To obtain an estimate of the ac anisotropy, we performed μSR measurements with the field both parallel and perpendicular to the c direction.[18] This gives an anisotropy of $\gamma = 4.3(2)$, in agreement with earlier determinations by SANS of 4.5(2).[14] This parameter will be used again in the discussion of the melting line.

The temperature dependence of the scattered neutron intensity, summed over all diffraction peaks, is shown for applied fields of 1 and 4 T in Fig. 4. The temperature well below T_c, at which the intensity falls to zero, is interpreted as the melting of the FLL.[4] In both cases the field was at 51° to the c axis. There are several interesting features in this figure. First, the scattered intensity is zero above the

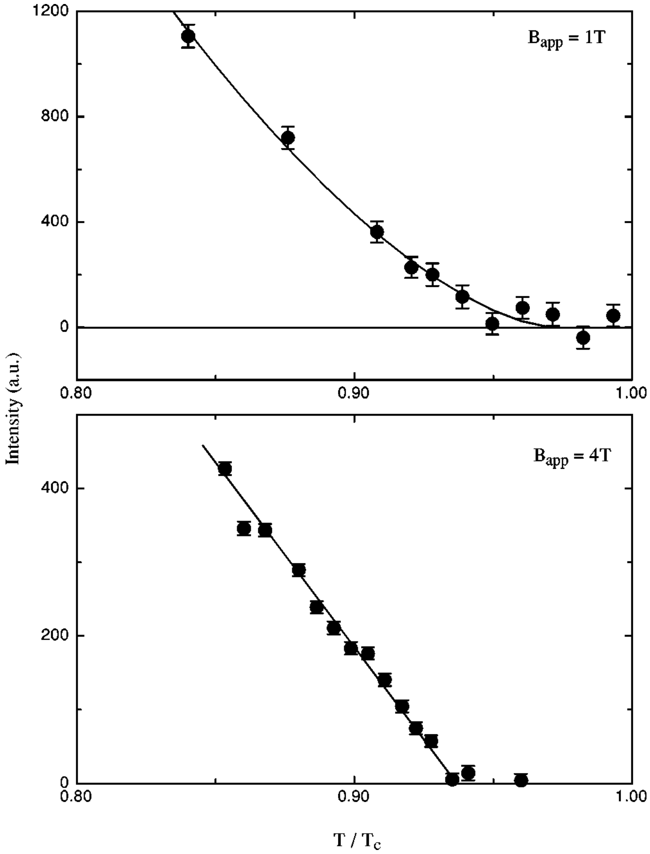

FIG. 4. Temperature dependence of the scattered intensity near the melting temperature at two different fields. Top, 1 T; bottom, 4 T. As can be seen, the intensity falls continuously to zero at the melting temperature consistent with a second-order transition to an entangled vortex liquid. As can be seen by comparing the two plots, the falloff at low fields is slower than at high fields (see the text).

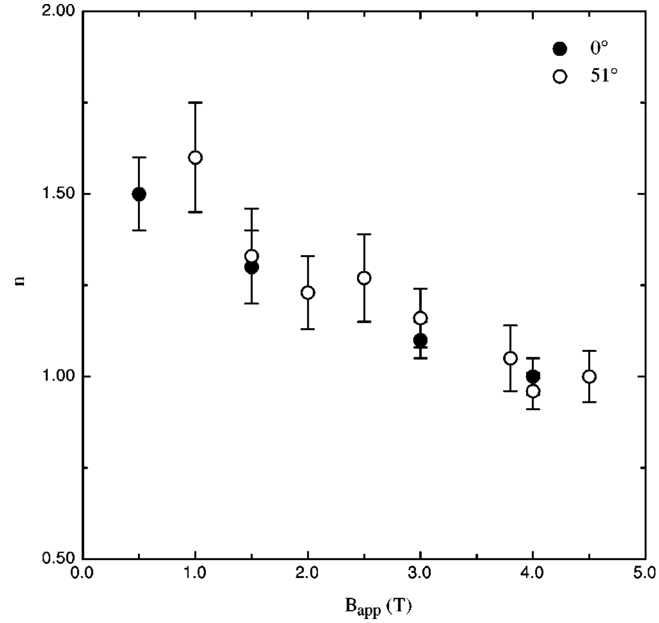

FIG. 5. Field dependence of the exponent n parametrizing the temperature dependence of the scattered intensity (see the text) for both orientations. This field dependence is in qualitative agreement with the field dependence of the jump in specific heat ΔC as given in Fig. 11 of Ref. 10. Such a field dependence might arise from a difference in thermal fluctuations at different fields, but no concise theoretical description could be found (see the text).

melting temperature. As is the case in BSCCO,[4] this is most probably due to the entanglement of the vortices (disorder along their length) above the melting temperature, which reduces the scattered intensity to zero. The observation of entangled (or decoupled) vortex lines has already been reported from measurements applying a current at the top of a sample, while recording the voltage difference on the bottom.[19] Above the irreversibility line, the voltage measured on the bottom of the sample drops to zero, indicating an entanglement of the vortices. This would also be in accord with numerical simulations,[20] which show a simultaneous occurrence of melting and entanglement.

The temperature dependence of the FLL signal below the melting temperature is different for the low-field data from the high-field data. We note that this temperature dependence will arise from two causes: (i) the variation of the superconducting penetration depth, which for a perfect FLL would give a temperature dependence of intensity according to Eqs. (2) and (3), $I(T)\propto 1/\lambda^4(T)$, and (ii) the variation of the FLL order as thermal destruction of the flux line structure increases with temperature. Clearly, the second term is the cause of the zero intensity as the flux lattice melts, but the first term will contribute to the temperature dependence below T_m, so we consider its contribution. The Ginzburg-Landau mean field picture gives a variation of the penetration depth as $\lambda(T)=\lambda(0)(1-t)^{1/2}$. If we assume that λ is little affected by our applied fields, which are much less than the mean field H_{c_2} at the melting temperature, then this gives $I(t)=I_0(1-t)^2$. However, it appears from microwave measurements at zero field[21] that critical fluctuations renormalize the temperature dependence of the penetration depth to $\lambda(T)=\lambda(0)(1-t)^{1/3}$; this is the dependence expected in the three-dimensional (3D) XY model and gives $I(t)=I_0(1-t)^{4/3}$. Whatever the functional dependence of $\lambda(T)$, unless it tends to infinity at the melting temperature, it will not affect the temperature dependence *very close* to T_m: This will be controlled by the FLL order. Hence it is of some importance to note that within our experimental error, the intensity falls to zero *continuously* at T_m, implying that the transition is not of first order. At 4 T the FLL intensity falls to zero approximately linearly with temperature, while the falloff is much more gradual at 1 T. This can be quantified by fitting a power law of the form $I(t)=I_0(1-t/t_m)^n$, where n parametrizes the shape of the temperature dependence and is ~ 1 at 4 T and ~ 1.5 at 1 T. If we regard the scattered intensity as the square of a phenomenological FLL order parameter, then at 4 T the intensity surprisingly follows the temperature dependence expected for an order parameter in mean field theory. At low fields, however, this is not the case. Since we do not know of a detailed theory for these results, we confine ourselves to reporting the rest of our data in terms of the power law $I\propto(1-t/t_m)^n$ that best describes the variation of the intensity below T_m. The results are summarized by Fig. 5, where we see a general trend to smoother transitions at low fields.

It is interesting to compare this field dependence with that of the jump observed in specific heat (Fig. 11 in Ref. 10). For their sample with $x=0.03$, which is very similar to the one studied here, the step shows a comparable qualitative dependence. ΔC in that sample is almost field independent at fields above 5 T and then decreases below fields ~ 3 T, until the jump cannot be resolved at fields lower than 1.5 T. This corresponds to our observation of the field dependence of the exponent n, being field independent above ~ 4 T and increasing at lower fields. Viewing the scattered intensity as a FLL order parameter as discussed above, an increasing exponent n corresponds to a smaller change in the slope of the order parameter at the melting transition. Thus a bigger exponent n corresponds to a smaller jump in specific heat, consistent with the observation.

As already mentioned, the melting transitions that we observe are apparently continuous. Such a behavior is consistent with a second-order phase transition, as observed in similar crystals by Roulin *et al.*, using specific heat measurements single crystals,[7] where DTA measurements demonstrate the existence of a first-order transition. Similar results are also found in specific heat measurements on ultrahigh-purity twinned YBCO crystals,[9] where a peak in specific heat was found at intermediate fields. Moreover, in SANS experiments on a large untwinned crystal (with very few remaining twin planes), show a much sharper transition than those presented here[22] at high fields. Although no clear jump in neutron intensity, as expected for a first-order transition, could be found in that sample, the data are not inconsistent with a smeared first-order transition.

A second-order transition, as observed in this and an other work,[10] has been predicted for the melting of a vortex glass.[1,23] The glass transition line is predicted to scale[1] as $B_G \propto \xi^{-2}$, where ξ is the coherence length with a temperature dependence of the form $\xi(T)=\xi_0(1-t)^{-\nu}$, where $\nu=1/2$ in the mean field approximation and $\nu=2/3$ in the 3D XY model. This results in a scaling for the melting line as

$$B_G \propto (1-t)^{4/3} \tag{5}$$

in the limit where the 3D XY model is applicable. However, as we observe a diffraction pattern the supposed vortex glass has to be what is called a ''weak glass'' or ''Bragg glass.''[24] It is thus rather surprising that such weak glassiness may turn the first-order transition expected for an ideal lattice into a second-order transition. The different available data[22,7,9,10] seem to indicate that not only the twin planes, but also the degree of purity may be important in modifying the order of the transition.

In a twinned crystal containing no green phase, Junod *et al.*[9] observed a melting line of first or second order depending on the applied field. Similarly, DTA measurements on untwinned crystals[7] find no latent heat at the melting transition in low fields ($B<0.5$ T), indicating that there is either no transition or a second-order transition at low fields. Moreover, the first-order (high-field) and second-order (low-field) transitions found in Ref. 9 lie on the same phase line, indicating a single process.

Setting aside the nature of the transition, we may still obtain predictions as to the position of the melting line in a B-T phase diagram using a Lindemann approach. The Lindemann criterion for the melting of a lattice involves calculating the thermal fluctuations of the lattice. When these fluctuations reach a certain fraction of the lattice constant, the phase transition is thought to occur. This leads to a criterion for melting

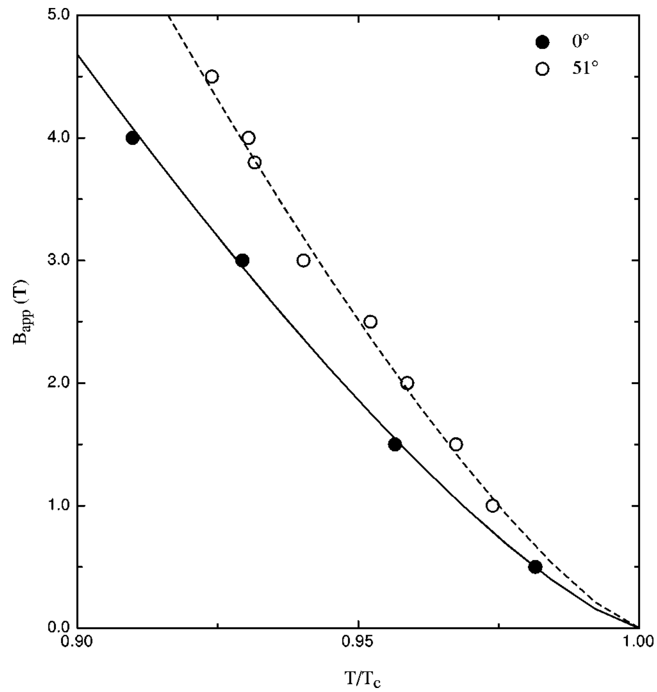

FIG. 6. Melting lines as determined from the temperature dependences of the scattered intensities for both orientations (filled circles, $\vartheta=0°$; open circles, $\vartheta=51°$). The lines through the data correspond to a fit to Eq. (7), yielding a value for the Lindemann number of $c_L=0.15$. The data for the field parallel to c differ slightly from the expected angular scaling [see Eq. (8)]. This is probably due to pinning by twin planes (see the text).

$$\langle u^2(T)\rangle = c_L^2 a_0^2, \tag{6}$$

where $c_L \simeq 0.1$–0.2 is the Lindemann number and $a_0 \sim (\Phi_0/B)^{1/2}$ is the intervortex distance. Calculating the thermal fluctuations using the (dispersive) elastic constants of a FLL then leads to the expression[23,25]

$$B_m(T) \simeq \frac{\Phi_0^5 c_L^4}{[1.5\pi\gamma k_B T \lambda(T)^2]^2}, \tag{7}$$

where k_B is Boltzmann's constant. Using the temperature dependence of the penetration depth in the 3D XY model presented earlier, this gives a similar temperature dependence of the melting temperature to that predicted for the vortex-glass transition [see Eq. (5)]. For temperatures close to T_c, where the 3D XY model is applicable and the $1/T$ in Eq. (7) may be regarded as constant, the two predictions are exactly the same and cannot be distinguished. At higher fields, however, where $1/T$ becomes important and mean field theory might be applicable, the two theories predict different melting lines. Such fields are, however, beyond our range of measurement.

Figure 6 shows the melting temperatures, as determined from the point above which the scattered intensity disappears, for both orientations studied. The line through the data is a fit to $B_m = B_0(1-t)^{4/3}$, corresponding to Eq. (7). According to the anticipated angular scaling for the melting line,

$$B_m(\vartheta) = B_m(0)/[\cos^2(\vartheta) + 1/\gamma^2 \sin^2(\vartheta)]^{1/2}, \qquad (8)$$

the prefactors in the two orientations are expected to differ by a factor of $B_0(0)/B_0(51) = 0.66$ (assuming $\gamma = 4.2$; see above). From the fitted values $B_0(0) = 100(10)$ T and $B_0(51) = 135(10)$ T, we obtain 0.74(9), in fair agreement with the prediction. Taking into account the values for the anisotropy and the penetration depth as determined by μSR,[18] we can then determine the Lindemann number to be $c_L = 0.15$, also in reasonable agreement with theoretical expectations. It should be noted, however, that Kwok *et al.*[2] find an angular dependence of the melting temperature showing a cusp around $\vartheta = 0$. In contrast to these transport measurements however, SANS and specific heat measurements[10] find a clear melting transition for fields parallel to the c direction, not inconsistent with the angular scaling observed in untwinned crystals.[22,7,26] The fact that the ratio of prefactors we obtain is somewhat bigger than expected might nevertheless arise from the strong pinning properties of the twin planes. A similar trend can be found in the data of Roulin *et al.*,[10] who determine the anisotropy from the melting line and the upper critical field B_{c_2} parallel and perpendicular to the c axis. The anisotropies determined from the melting line are consistently smaller than those determined from B_{c_2}, but as in the case presented here the experimental uncertainty is too large for a quantitative discussion of such a small effect. It is possible that in the presence of twin plane pinning, SANS and specific heat measurements give a better indication of melting than transport measurements because the former tell us about *equilibrium thermodynamic* properties of the system. Considering that the structure of the FLL is mainly determined by the twin planes (see Figs. 2 and 3) it is surprising, however, that the twin planes do not have a stronger influence on the melting temperatures.

IV. CONCLUSIONS

In conclusion, we have presented SANS measurements of the melting of the FLL in heavily twinned YBCO. The data are consistent with a recent specific heat study on crystals with similar twinning and purity.[10] The findings are consistent with a second-order phase transition, at a phase boundary as predicted by a Lindemann criterion. The observed melting line also shows the field and temperature dependence expected for a vortex-glass melting line as predicted from the 3D *XY* model. With the limited range of fields studied we are not able to distinguish between the two theoretical predictions. The effect of the twin-plane boundaries and the superconducting anisotropy on both the melting line and the FLL structure were studied by applying the field parallel to the c direction and at an angle of 51°. It was found that the lattice structure is strongly influenced, with the diffraction pattern showing a fourfold symmetry (but not a fourfold lattice) for the field parallel to c, whereas two distorted hexagonal lattices are found for the field at 51°. In contrast, the melting line is only very slightly affected by the presence of the twin planes, consistent with the findings of specific heat measurements.[10]

Finally, we find unexpected behavior in the temperature dependence of the scattered intensity close to the melting temperature. The temperature dependence of the scattered intensity, as parametrized by the exponent n, depends on the applied field, falling more rapidly (decreasing n) with increasing field. This behavior is reminiscent of that observed by heat capacity measurements on a similar sample,[10] where the jump in heat capacity at the melting transition rises with field. However, in both these cases, the results reflect the temperature dependence of not only the FLL structure, but also the underlying superconducting parameters, such as the penetration depth and the coherence length.

ACKNOWLEDGMENTS

We would like to thank Tim Armstrong for providing the sample and Michel Bonnaud (ILL) for technical support. Discussions with Marlyse Roulin on our and her results were appreciated. Financial support from the EPSRC of the United Kingdom and the Swiss National Science Foundation is gratefully acknowledged. This work was funded in part by Oak Ridge National Laboratory, which is managed by Lockheed Martin Energy Research Corporation under Contract No. DE-AC05-96OR22464 for the U.S. DOE.

*Present address: Laboratoire de Physique des Solides, Bâtiment 510, Université Paris–Sud, 91405 Orsay, France.

† Present address: The Institute of Physics, 76 Portland Place, London W1N 4AA, United Kingdom.

[1] D. S. Fisher, M. P. A. Fisher, and D. A. Huse, Phys. Rev. B **43**, 130 (1991).

[2] W. K. Kwok, S. Fleshler, U. Welp, V. M. Vinokur, J. Downey, G. W. Crabtree, and M. M. Miller, Phys. Rev. Lett. **69**, 3370 (1992).

[3] P. L. Gammel, L. F. Schneemeyer, J. V. Waszczak, and D. J. Bishop, Phys. Rev. Lett. **61**, 1666 (1988); H. Safar, P. L. Gammel, D. A. Huse, D. J. Bishop, J. P. Rice, and D. M. Ginsberg, *ibid.* **69**, 824 (1992); D. E. Farrell, J. P. Rice, and D. M. Ginsberg, *ibid.* **67**, 1165 (1991).

[4] R. Cubitt, E. M. Forgan, G. Yang, S. L. Lee, D. McK. Paul, H. A. Mook, M. Yethiraj, P. H. Kes, T. W. Li, A. A. Menovsky, Z. Tarnawski, and K. Mortensen, Nature (London) **365**, 407 (1993).

[5] S. L. Lee, P. Zimmermann, H. Keller, M. Warden, I. M. Savić, R. Schauwecker, D. Zech, R. Cubitt, E. M. Forgan, P. H. Kes, T. W. Li, A. A. Menovsky, and Z. Tarnawski, Phys. Rev. Lett. **71**, 3862 (1993).

[6] S. L. Lee, C. M. Aegerter, H. Keller, M. Willemin, B. Stäuble-Pümpin, E. M. Forgan, S. H. Lloyd, G. Blatter, R. Cubitt, T. W. Li, and P. Kes, Phys. Rev. B **55**, 5666 (1997).

[7] A. Schilling, R. A. Fisher, N. E. Phillips, U. Welp, W. K. Kwok, and G. W. Crabtree, Nature (London) **382**, 791 (1996); Phys. Rev. Lett. **78**, 4833 (1997).

[8] M. Roulin, A. Junod, and E. Walker, Science **273**, 1210 (1996).

[9] A. Junod, M. Roulin, J.-Y. Genoud, B. Revaz, A. Erb, and E.

Walker, Physica C **275**, 245 (1997).

[10] M. Roulin, A. Junod, and E. Walker (unpublished); M. Roulin (private communication).

[11] E. M. Forgan and S. L. Lee, Phys. Rev. Lett. **75**, 1422 (1995).

[12] M. B. Walker and T. Timusk, Phys. Rev. B **52**, 97 (1995).

[13] B. Keimer, W. Y. Shih, R. W. Erwin, J. W. Lynn, F. Dogan, and I. A. Aksay, Phys. Rev. Lett. **73**, 3459 (1994); Science **262**, 83 (1993).

[14] M. Yethiraj, H. A. Mook, G. D. Wignall, R. Cubitt, E. M. Forgan, D. McK. Paul, and T. Armstrong, Phys. Rev. Lett. **70**, 857 (1993); **71**, 3019 (1993).

[15] M. T. Wylie, E. M. Forgan, S. H. Lloyd, S. Lee, R. Cubitt, M. Yethiraj, and H. A. Mook, Czech. J. Phys. Suppl. **46**, 1569 (1996).

[16] E. M. Forgan, D. McK. Paul, H. A. Mook, P. A. Timmins, H. Keller, S. Sutton, and J. S. Abell, Nature (London) **343**, 735 (1990).

[17] D. Cribier, B. Jacrot, L. Madhov Rao, and B. Farnoux, Phys. Lett. **9**, 106 (1964).

[18] C. M. Aegerter, E. M. Forgan, and S. L. Lee (unpublished).

[19] H. Safar, E. Rodriguez, F. de la Cruz, P. L. Gammel, L. F. Schneemeyer, and D. J. Bishop, Phys. Rev. B **46**, 14 238 (1992).

[20] H. Nordborg and G. Blatter, Phys. Rev. Lett. **79**, 1925 (1997).

[21] S. Kamal, D. A. Bonn, N. Goldenfeld, P. J. Hirschfeld, R. Liang, and W. N. Hardy, Phys. Rev. Lett. **73**, 1845 (1994).

[22] C. M. Aegerter, E. M. Forgan, S. H. Lloyd, S. T. Johnson, R. Cubitt, S. L. Lee, D. McK. Paul, M. Yethiraj, A. Rykov, and S. Tajima (unpublished).

[23] G. Blatter, M. V. Feigelman, V. B. Geshkenbein, A. I. Larkin, and V. M. Vinokur, Rev. Mod. Phys. **66**, 1125 (1995).

[24] T. Giamarchi and P. Le Doussal, Phys. Rev. Lett. **72**, 1530 (1994); Phys. Rev. B **52**, 1242 (1995).

[25] A. Houghton, R. A. Pelcovits, and A. Sudbø, Phys. Rev. B **40**, 6763 (1989).

[26] A. Schilling (private communication).